Kalman Filters Unifying Model-based and HF Injection-based Sensorless Control of PMSM Drives

Václav Šmídl
Institute of Information Theory and Automation
Prague, Czech Republic
email: `smidl@utia.cas.cz`

David Vošmik, Zdeněk Peroutka
Regional Innovation Centre for Electrical Engineering
University of West Bohemia
Pilsen, Czech Republic
email: `peroutka@ieee.org`

Abstract—Methods of sensorless control of PMSM drives are commonly divided into model-based and high-frequency injection based approaches. Each of these approaches uses a different algorithm for estimation of the rotor position and speed. Typically a Kalman filter is used for the model-based approach and phase-locked loop (PLL) for the hf injection based approach. In this paper, we show that the PLL is a steady state solution of the Kalman filter for a special state space model. Since this model has a commonly used state equations, we can easily combine the observation equations from the model-based approach with those from the hf injections. Several possibilities of combination are described and tested in the paper. We illustrate properties of these algorithms on experimental data in sensored mode. Sensorless control strategy based on the presented models is demonstrated on a laboratory prototype of surface mounted permanent magnet synchronous motor (PMSM) drive of rated power of 10.7kW.

I. INTRODUCTION

Techniques for sensorless control of an ac drive—i.e. its operation without either rotor position and/or speed sensor—has been traditionally split into model-based approaches and anisotropy approaches based on analysis of superimposed artificial testing signal of known frequency (hf injections). Typical examples of the model based techniques are MRAS [1], the Extended Kalman Filter (EKF) [2], [3], or the unscented Kalman filter [4]. Typical examples of high-frequency injections are sinusoid signal injection evaluated via the phase locked loop (PLL), e.g. for injections in rotating reference frame [5], and its various modifications [6], [7], [8]. The model based approaches are more reliable in the high speed regimes while the anisotropy based approach is superior in the low speed range and especially in the standstill. This is the reason for derivation of switching schemes (often called hybrid estimators) [9].

The two basic approaches to sensorless control are perceived as two incompatible phenomena. In this paper, we show that they are actually closely related. The phase lock loop is known to be a simplification of the Kalman filter for a simple state-space model [10], with explicit transformation between their coefficients given in [11]. We show that this state space model of the PLL is also commonly used in model based approaches. However, the model based techniques use different observation equations. Since the state space models allows to combine any number of observation models, we design a new state-space model that combines the observation models of both

approaches. Similar approach was proposed in [12].

The new state-space model is tested on a PMSM prototype of rated power of 10.7kW. We demonstrate properties of the hf injection techniques in simulation on recorded data and the final algorithm in experimental study on a real drive.

II. MATHEMATICAL MODELS OF PMSM

A commonly used model of a PMSM is mathematical model in rotating reference frame linked to a rotor flux linkage vector [13]:

$$\frac{di_d}{dt} = \frac{1}{L_d}(-R_s i_d + L_q i_q \omega + u_d), \tag{1}$$

$$\frac{di_q}{dt} = \frac{1}{L_q}(-R_s i_q - L_d i_d \omega - \Psi_{pm}\omega + u_q), \tag{2}$$

$$\frac{d\omega_{me}}{dt} = \frac{1}{J}[k_p p_p^2((L_d - L_q)i_d i_q + \Psi_{pm}i_q) - B\omega_{me}], \tag{3}$$

$$\frac{d\vartheta_{me}}{dt} = \omega_{me}. \tag{4}$$

Here, i_d, i_q, u_d and u_q represent components of stator current and voltage vector in the rotating reference frame, respectively; ω_{me} is electrical rotor speed and ϑ_e is electrical rotor position. Parameters of the model are stator inductances in axis d and q, L_{sd} and L_{sq}, stator resistance R_s, flux linkage excited by permanent magnets on the rotor Ψ_{pm}, moment of inertia J, friction coefficient B, the number of pole pairs p_p, the Park constant k_p.

This model is universally valid, however, it is unsuitable for use in digital controllers with uniform sampling time. Various conversions to discrete time has been proposed, we review two basic approaches.

A. Euler discretization

A common approach is to apply the first-order Euler formula to (1)–(4) for time step Δt:

$$i_{d,t+1} = a_d i_{d,t} + b_d i_{q,t}\omega_t + c_d u_{d,t} + \epsilon_{d,t}, \tag{5}$$

$$i_{q,t+1} = a_q i_{q,t} - f_q \omega_t - b_q i_{d,t}\omega_t + c_q u_{q,t} + \epsilon_{q,t}, \tag{6}$$

$$\omega_{me,t+1} = \omega_{me,t} + e_q i_{q,t} + e_{dq}i_{d,t}i_{q,t} + \epsilon_{\omega,t}, \tag{7}$$

$$\vartheta_{e,t+1} = \vartheta_{e,t} + \omega_{me,t}\Delta t + \epsilon_{\vartheta,t}. \tag{8}$$

Here, parameters of the model have been aggregated in constants $a_d = (1 - \frac{R_s}{L_{sd}}\Delta t)$, $a_q = (1 - \frac{R_s}{L_{sq}}\Delta t)$, $b_d = \frac{L_{sq}}{L_{sd}}\Delta t$, $b_q =$

$\frac{L_{sd}}{L_{sq}}\Delta t$, $c_d = \frac{\Delta t}{L_{sd}}$, $c_q = \frac{\Delta t}{L_{sq}}$, $f_q = \frac{\Psi_{pm}}{L_{sq}}\Delta t$, $e_q = \frac{1}{J}k_p p_p^2\Psi_{pm}$, and $e_{dq} = \frac{1}{J}k_p p_p^2(L_d - L_q)$. Noise terms $\epsilon_{d,t}, \epsilon_{q,t}, \epsilon_{\omega,t}, \epsilon_{\vartheta,t}$, aggregate errors caused by inaccurate discretization, uncertainties in parameters (e.g. due to temperature changes, saturation), unobserved physical effects (such as the unknown load, dead-time effects, non-linear voltage drops on power electronics devices).

Equations (5)–(8) can be used to design a non-linear state-space model of PMSM in two ways: (i) full model with state vector $x_t = [i_{d,t}, i_{q,t}, \omega_{me,t}, \vartheta_{e,t}]$, [3], where (5)–(8) being state equations, and observation equations $\bar{i}_{d,t} = i_{d,t} + \epsilon_{i,d}$, $\bar{i}_{q,t} = i_{q,t} + \epsilon_{i,q}$, or (ii) reduced order model with state vector $x_t = [\omega_{me}, \vartheta_{e,t}]$, [14], where state equations are (7)–(8), and observation equations are (5)–(6), where $i_{d,t}$ are replaced by delayed observations. Alternatively, the rotor speed equation can be simplified to yield a simple state equation

$$\begin{bmatrix} \omega_{me,t+1} \\ \vartheta_{e,t+1} \end{bmatrix} = \begin{bmatrix} 1 & \\ \Delta t & 1 \end{bmatrix} \begin{bmatrix} \omega_{me,t} \\ \vartheta_{e,t} \end{bmatrix}. \quad (9)$$

Both models are used in model-based approaches, typically in the Extended Kalman filter (EKF).

B. Analytical solution for hf injections

Instead of direct discretization, differential equations (1)–(2) can be solved analytically under the following conditions

$$\omega \simeq 0,$$
$$\mathbf{u}_c = u_{inj}\cos(\omega_{inj}t)\exp(j(\vartheta_{inj} - \vartheta_{me})),$$

where $\mathbf{u}_c$ is the vector of the injected voltage in rotating reference frame, u_{inj} is the amplitude of the injected hf voltage, ω_{inj} its frequency and ϑ_{inj} is the angle of the injected signal. Then the vector of the stator currents in the rotating reference frame is [5]:

$$\mathbf{i}_{inj} = \frac{u_{inj}}{\omega_{inj}}\sin(\omega_{inj}t)\times$$
$$\left(\frac{1}{L_d}\cos(\vartheta_{inj} - \vartheta_{me}) + j\frac{1}{L_q}\sin(\vartheta_{inj} - \vartheta_{me})\right).$$

After algebraic manipulation, the currents can be written as

$$i_{inj,q} = i_{inj,d}\frac{L_d}{L_q}\tan(\vartheta_{inj} - \vartheta_{me}), \quad (10)$$

where $i_{inj,q}, i_{inj,d}$ are projections of the current vector into the d and q axis. This model is commonly used in the hf injection methods [5], [9], with the following simplification

$$i_{inj,q} = i_{inj,d}\frac{L_d}{L_q}\sin(\vartheta_{inj} - \vartheta_{me}), \quad (11)$$

which is valid when the difference $(\vartheta_{inj} - \vartheta_{me})$ is small, and $\cos(\vartheta_{inj} - \vartheta_{me}) \approx 1$.

III. EXTENDED KALMAN FILTER

The Extended Kalman filter (EKF) is a state estimator of general state space models

$$x_{t+1} = f(x_t, u_t) + \xi_x,$$
$$y_t = h(x_t, u_t) + \xi_y, \quad (12)$$

where x_t is the state vector, y_t is the vector of measurements, $f(x_t, u_t)$ and $h(x_t, u_t)$ is a non-linear equation of the state evolution and measurement equation, respectively. The model errors ξ_x, ξ_y are assumed to be zero mean Gaussian with variances Q and R respectively. The EKF provides the estimate of the state $\hat{x}_t$ as follows:

$$\hat{x}_t = f(\hat{x}_{t-1}) + K(y_t - h(\hat{x}_{t-1})). \quad (13)$$
$$R_y = CP_{t-1}C' + R_t, \quad (14)$$
$$K = S_{t-1}C'R_y^{-1}, \quad (15)$$
$$P_t = S_{t-1} - S_{t-1}C'R_y^{-1}CS_{t-1}, \quad (16)$$
$$S_t = AP_tA' + Q_t. \quad (17)$$

where $A = \frac{d}{dx_t}f(x_t, u_t)|_{\hat{x}_t}$, $C = \frac{d}{dx_t}h(x_t, u_t)|_{\hat{x}_t}$ are matrices of derivatives of the nonlinear model (12).

A. EKF for hf injections

Consider a reduced order state vector $x_t = [\omega_{e,t}, \vartheta_{me,t}]$ with state model (9) and observation equation (11). The matrices of derivatives are

$$A = \begin{bmatrix} 1 & \\ \Delta t & 1 \end{bmatrix}, \quad C = [0, -i_{inj,d,t}\frac{L_d}{L_q}\cos(\vartheta_{inj,t} - \vartheta_{me,t})], \quad (18)$$

Application of the general Kalman filtering equations (13)–(17) yields

$$\hat{\omega}_{e,t} = \hat{\omega}_{e,t-1} + k_{1,t}\Delta i_t, \quad (19)$$
$$\hat{\vartheta}_{me,t} = \hat{\vartheta}_{me,t-1} + \Delta t\hat{\omega}_{e,t-1} + k_{2,t}\Delta i_t \quad (20)$$
$$\Delta i_t = (i_{inj,q,t} - i_{inj,d}\frac{L_d}{L_q}\sin(\vartheta_{inj} - \hat{\vartheta}_{me})). \quad (21)$$

where $K = [k_1, k_2]^T$. Substituting (19) into (20) recursively yields

$$\hat{\vartheta}_{me,t} = \hat{\vartheta}_{me,t-1} + \Delta t\, k_1\sum_{\tau=1}^{t}\Delta i_\tau + k_2\Delta i_t, \quad (22)$$

which is an equation of a PI controller with input Δi_t, proportional constant k_2, and integration constant $\Delta t\, k_1$. Since k_1, k_2 are functions of $i_{inj,d}$, they can not be static. Introducing gains $\bar{k}_1 = k_1/i_{inj,d}$, $\bar{k}_2 = k_2/i_{inj,d}$, the proportional term (21) can be rewritten as

$$k_{2,t}\Delta i_t = \bar{k}_2(i_{inj,d,t}i_{inj,q,t} - i_{inj,d}^2\frac{L_d}{L_q}\sin(\vartheta_{inj} - \hat{\vartheta}_{me})), \quad (23)$$
$$\approx \bar{k}_2(i_{inj,d,t}i_{inj,q,t}) \approx \bar{k}_2(i_{inj,d,t}\text{sign}(i_{inj,q,t})) \quad (24)$$

and similarly for the integral term in (22).

The resulting equation for the rotor position estimation has the same structure as the PI PLL, Figure 1 (with the commonly
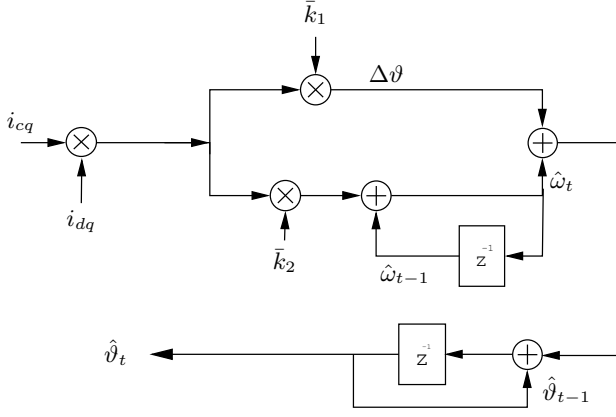
Figure 1. Signal flow of the EKF for hf-injections (and also for the proportional integral PLL).

used simplification (24)). In effect, the EKF adaptively tunes of the gains of the PI controller in the PLL. This fact has been noted in [10] for a model with constant matrix C. In such a case the relation between the coefficients of the EKF and that of the PI controller can be explicitly calculated [11].

We note the following:

- The current vector $\mathbf{i}_{inj}$ is not directly observable. A good reconstruction is obtained using band-pass filter. The choice of the filter may influence properties of the resulting algorithm significantly.
- Important advantage of equation (11) is that it is insensitive to the exact amplitude and distortion of the injected signal. Hence, the hf injection based methods are valued for their insensitivity to these parameters.
- Note however, that the presented EKF formulation has one substantial difference. The requirement of the closeness of ϑ_{inj} and ϑ_{me} is needed only with simplified model (11). The EKF for the original model (10) is no longer closely related to the PLL. In fact, it is more general, since the angle of the injected signal can be arbitrary. However, this algorithm is very sensitive to the choice of the band-pass filter and we will not use it.

B. EKF for a hybrid model

Many variants of the EKF has been proposed using various combinations of the state-space models (5)–(8). A very straightforward combination of the two techniques is to use the reduced order state model:

$$\omega_{me,t+1} = \omega_{me,t} + e_q i_{q,t} + e_{dq} i_{d,t} i_{q,t} + \epsilon_{\omega,t}, \qquad (25)$$

$$\vartheta_{e,t+1} = \vartheta_{e,t} + \omega_{me,t}\Delta t + \epsilon_{\vartheta,t}. \qquad (26)$$

and observation models of both the model-based and the hf injection approaches:

$$i_{d,t} = a_d i_{d,t-1} + b_d i_{q,t-1}\omega_{t-1} + c_d u_{d,t-1} + \epsilon_{d,t}, \qquad (27)$$

$$i_{q,t} = a_q i_{q,t-1} - (f_q + b_q i_{d,t-1})\omega_{t-1} + c_q u_{q,t-1} + \epsilon_{q,t}, \qquad (28)$$

$$i_{inj,q} = i_{inj,d}\frac{L_d}{L_q}\sin(\vartheta_{inj} - \vartheta_{me}). \qquad (29)$$

Here, $u_{d,t-1}, u_{q,t-1}$ are the requested voltages from the controller including the injected signal.

The matrices of the derivatives are:

$$A = \begin{bmatrix} 1 \\ \Delta t & 1 \end{bmatrix}, C = \begin{bmatrix} b_d i_{q,t-1} & 0 \\ -(f_q + b_q i_{d,t-1}) & 0 \\ 0 & C_{32} \end{bmatrix}, \quad (30)$$

$$C_{32} = -i_{inj,d,t}\frac{L_d}{L_q}\cos(\vartheta_{inj,t} - \vartheta_{me,t}). \qquad (31)$$

Which is a hybrid method combining observations from the hf injection and the model-based approach. This method offers the possibility to incorporate a band-pass filter commonly used in the hf injection approaches.

C. EKF for a combined model

An alternative combination of the Euler discretization and the analytical solution of the hf injection is [12]:

$$i_{d,t} = a_d i_{d,t-1} + b_d i_{q,t-1}\omega_{t-1} + c_d \overline{u}_{d,t-1} +$$
$$+ \frac{u_{inj}}{\omega_{inj}}\frac{1}{L_d}\cos(\vartheta_{inj} - \vartheta_{me})\sin(\omega_{inj}t) + \epsilon_{d,t}, \quad (32)$$

$$i_{q,t} = a_q i_{q,t-1} - (f_q + b_q i_{d,t-1})\omega_{t-1} + c_q \overline{u}_{q,t-1} +$$
$$+ \frac{u_{inj}}{\omega_{inj}}\frac{1}{L_q}\sin(\vartheta_{inj} - \vartheta_{me})\sin(\omega_{inj}t) + \epsilon_{q,t}, \quad (33)$$

where, the $\overline{u}_d, \overline{u}_q$ are the requested voltages without the injected hf signal. Equations (32)–(33) are an alternative observation model for state model (25)–(26). The matrix of derivatives of the observation model is:

$$C = \begin{bmatrix} b_d i_{q,t-1} & \frac{u_{inj}}{\omega_{inj}}\frac{1}{L_d}\sin(\vartheta_{inj} - \vartheta_{me})\sin(\omega_{inj}t) \\ -(f_q + b_q i_{d,t-1}) & -\frac{u_{inj}}{\omega_{inj}}\frac{1}{L_q}\cos(\vartheta_{inj} - \vartheta_{me})\sin(\omega_{inj}t) \end{bmatrix}.$$

The main advantage of this model is that it does not require the band-pass filter.

D. EKF for a loosely coupled model

In the reduced order state space model, (7)–(8), the rotor position and the rotor speed are closely coupled. An error in one quantity is thus immediately propagated to the other. From empirical observations, estimates of the rotor position in the standstill fluctuate around the true position. The coupling between speed and position implies that the rotor speed is also oscillating. This is an undesired effect, and we seek a way how to decouple estimate of the rotor speed from these fluctuations. We introduce an additional state variable $z_t = \vartheta_{inj} - \vartheta_{me}$, as a model of local fluctuation of the estimated rotor position:

$$\omega_{me,t+1} = \omega_{me,t} + \epsilon_{\omega,t},$$
$$\vartheta_{e,t+1} = \vartheta_{e,t} + \omega_{me,t}\Delta t + z_t + \epsilon_{\vartheta,t}, \qquad (34)$$
$$z_{t+1} = 0 + \epsilon,$$

where the predicted value of z_t is always zero, since the injections are aligned with the estimates. The observation equations are (27)–(28) and the following modification of (29):

$$i_{inj,q,t} = i_{ing,d,t}\frac{L_d}{L_q}\sin(z_t). \qquad (35)$$
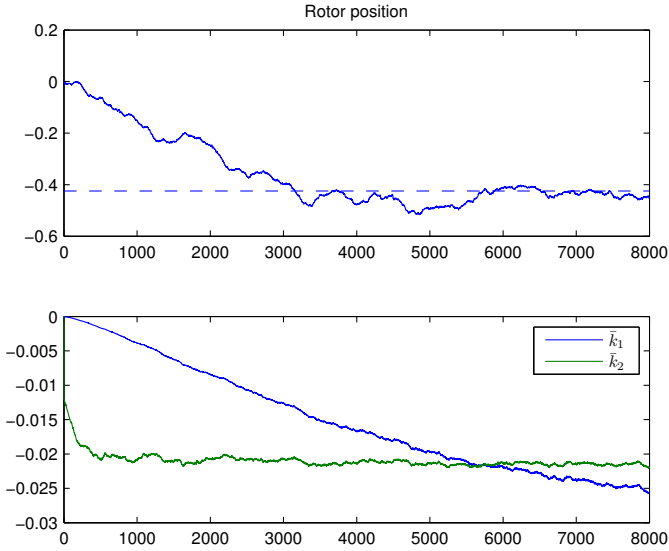
Figure 2. EKF for the PLL model from Section III-A on recorded data from the tested prototype at standstill.

The matrices of derivatives for the EKF are then

$$A = \begin{bmatrix} 1 & 0 & 0 \\ \Delta t & 1 & 1 \\ 0 & 0 & 0 \end{bmatrix}, C = \begin{bmatrix} b_d i_{q,t} & 0 & 0 \\ -(f_q + b_q i_{d,t}) & 0 & 0 \\ 0 & 0 & \frac{L_d}{L_q} i_{inj,d,t} \end{bmatrix}.$$

IV. SIMULATION STUDIES

For illustration of the properties of the EKF tuned PLL from Section III-A we run the algorithm of a set of data recorded on the tested drive prototype at standstill. The sampling period was 125μs, the frequency of the injected signal was ω_{inj}=1kHz and amplitude u_{inj}=7V.

The results are displayed in Figure 2 via the estimate of the rotor position ϑ_{me}, top, and the constant parts of the Kalman gain, $\bar{k}_1$ and $\bar{k}_2$ from (23). Note that the proportional gain has very short settling time and stays constant, the integral gain is converging to a stationary value much longer. For signals $i_{inj,q}$ and $i_{inj,d}$ filtered by a band-pass filter, the initial transient on the PI coefficients is not so smooth. This confirms that the PLL is a steady state solution of the Kalman filter.

V. EXPERIMENTAL RESULTS

A. Experiment setup

The drive control is based on the conventional vector control in Cartesian coordinates in rotating reference frame (d,q) linked to a rotor flux linkage vector. An input to the drive controller is the commanded electrical rotor speed ω_{mew} which is controlled by the PI controller R_ω. Output of R_ω is the demanded torque component I_{sqw} of the stator current vector. The torque (I_{sqw}) and flux (I_{sdw}) currents are controlled by the PI controllers R_{Isd} and R_{Isq}, respectively. The field weakening is secured by the PI controller R_{Urm} which controls the PWM modulation depth (signal U_{rm}) and commands the flux current I_{sdw}. The current controllers are supported by block "voltage calculation" (often referred to as

"decoupling") which computes the components of the required stator voltage vector in (d,q) frame using a simplified model of the PMSM in steady-state. The components of the stator current vector ($i_{s\alpha}, i_{s\beta}$) and the reconstructed stator voltage vector $u_{s\alpha}, u_{s\beta}$ in the stationary reference frame are inputs to the EKF estimators. The stator voltage vector is reconstructed from the measured dc-link voltage and a known switching combination of the voltage-source converter. The voltage-source converter employs a third-harmonic injected PWM with carrier frequency of 8kHz. The sampling frequency of all the EKFs as well as of the drive control has been set to 125μs.

The EKF output is the estimated electrical rotor speed $\hat{\omega}_{me}$ and the electrical rotor position $\hat{\vartheta}_e$. The covariance matrices of all tested variants of the EKF were considered to be time- and state-invariant and were obtained by manual tuning. The proposed sensorless drive control with all presented EKF algorithms were implemented in TI TMS320F28335 processor with core clock of 150 MHz. Execution time of the EKF with the basic model and with the combined model is 16μs, execution time of the other models is 28μs (longer time is caused by calculation of bandpass filters taking approximately 12 μs). The tests were performed on a laboratory prototype of PMSM drive of rated power of 10.7kW.

B. Open loop results

Open-loop operation of the drive was used to tune parameters of the model and of the filter. Even with the best tuned parameters, the model does not fit exactly with the measurements, see Figure 3, top left, where the estimated rotor position of the basic EKF is displayed. Note that the error in the position changes with position of the rotor. This result suggests that the symmetry of the model (1)–(2) is violated. The hf injections method does not suffer from this error and estimate the position reliably. An expected behavior of the EKF with the extended models is to correct this bias. Note that from all extensions presented in this paper, only the loosely coupled model (Section III-D), is able to correct this error. The hybrid model (Section III-B) has almost constant error, and the combined model (Section III-C) has only negligible difference from the basic Kalman filter model. Since the combined model was reported to yield reliable performance on a different drive [12], these results suggest that performance of various extensions may significantly depend on the tested prototype.

C. Sensorless control

Closed loop operation of the tested algorithm was achieved by replacement of the observed rotor position by its estimates $\hat{\vartheta}_e$ from all methods. The rotor speed was reconstructed using numerical derivative of the position estimates $\hat{\vartheta}_e$ with sampling interval 12.5ms. Due to the presence of the hf injection, the position is estimated reliably and the drive can be controlled without a sensor in standstill and very low speed. This is demonstrated in Fig. 4 by a start and speed reversal at 0.13Hz. At this speed the estimation is dominated by contribution from the hf injection equation.
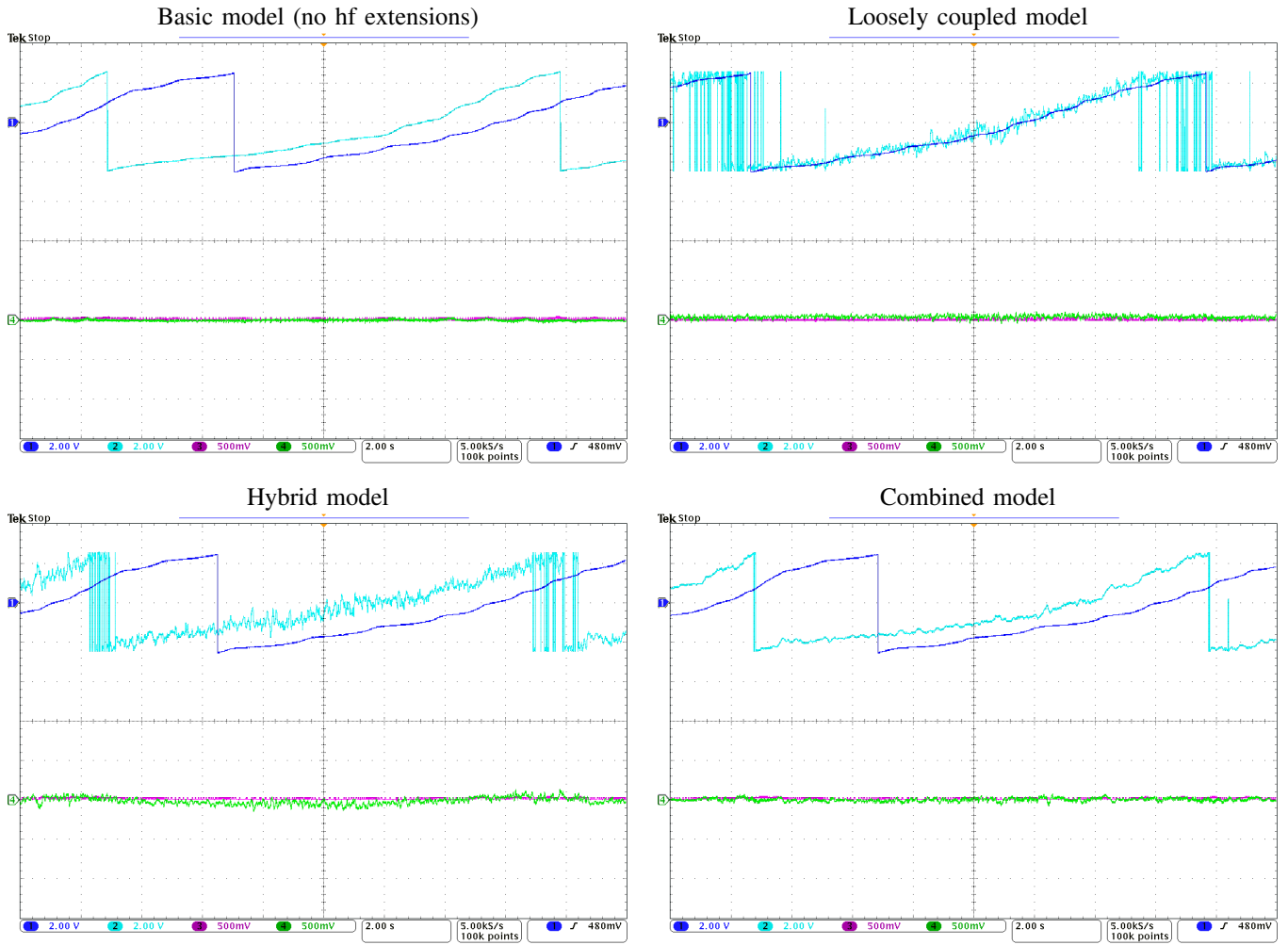
Figure 3. Experimental result at sensored mode of the drive control, el. speed of the drive is 1/15 Hz. Comparison of EKF estimates for different models. **ch1**: electrical rotor position (sensor) [144 deg/div], **ch2**: estimated electrical rotor position (EKF) [144 deg/div], **ch3**: electrical rotor speed (sensor) [4 Hz/div], **ch4**: estimated el. rotor speed (EKF) [4 Hz/div], time scale: 2 s/div

With increasing speed, contribution from the "model-based" observation equations increases and the estimates are still reliable. Performance of the selected sensorless control algorithms is demonstrated in speed reversal in Fig. 5 for the loosely coupled model (left) and for the combined model (right). The commanded electrical rotor speed followed a rectangular speed profile of ±4 Hz.

VI. CONCLUSION

We have studied state-space models of the PMSM drive for different discretization of the differential equation describing a PMSM drive. We have designed a special state-space model for which the EKF algorithm coincides with the proportional integral phase-locked loop algorithm commonly used to evaluate the injected hf signal. Key advantage of this state-space formulation is that it allows for combination of the equations used in model-based approaches with those used in the hf injection based techniques. We proposed several such equations, one of them has already been tested in a slightly different form. We have shown that the additional observation

equations from the hf injections is capable to compensate model mismatch of the model-based approaches at very low speeds. However, strong coupling between the rotor speed and the rotor position did not allow to compensate the error sufficiently. Only the proposed loosely coupled model was able to estimate the rotor position with accuracy comparable to that of the hf injection based methods. This model was also found to be able to secure sensorless operation of the drive at very low speed and standstill.
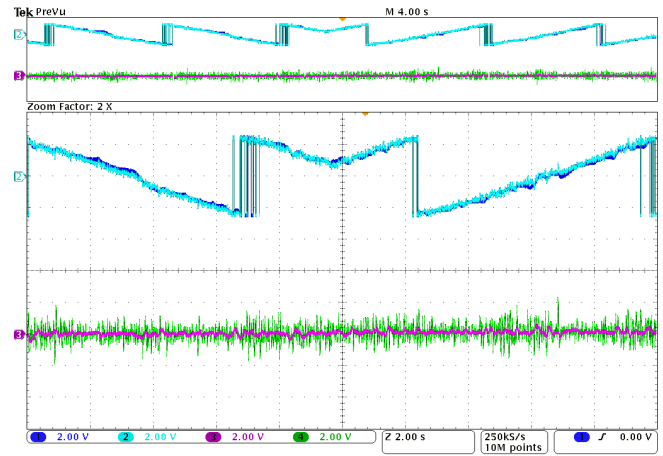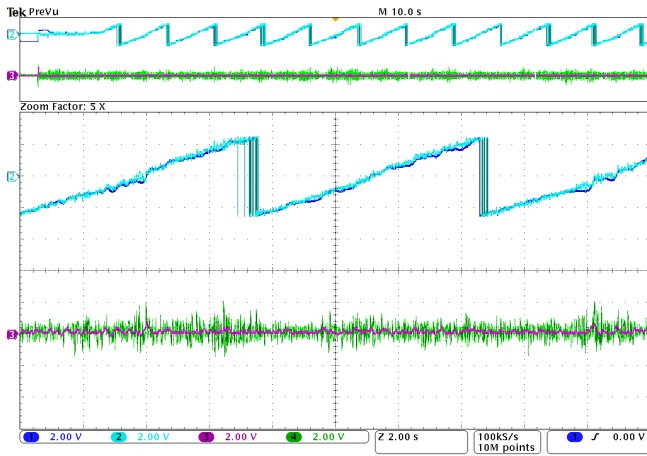
Figure 4. Sensorless mode – EKF using loosely coupled model. **Left:** start of the drive to el. speed of 0.13Hz, **Right**: speed reversal of $\pm$0.13Hz. **ch1**, **ch2**: electrical rotor position (sensor, EKF, respectively) [144 deg/div], **ch3**, **ch4**: electrical rotor speed (sensor, EKF, respectively) [4 Hz/div], time scale: 2 s/div.
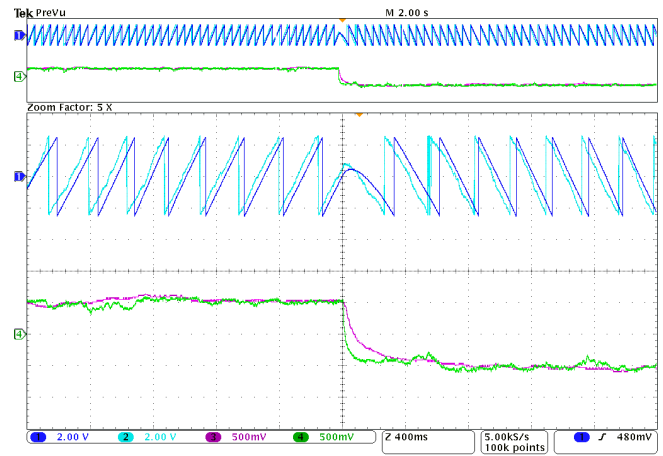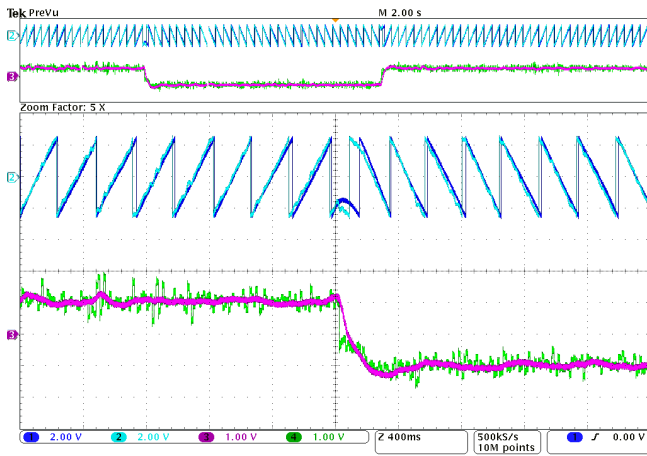
Figure 5. Experimental result – sensorless mode of the drive control with rectangular speed profile of $\pm$4Hz. **Left:** EKF with loosely coupled model. **Right**: EKF with combined model. **ch1**: electrical rotor position (sensor) [144 deg/div], **ch2**: estimated electrical rotor position (EKF) [144 deg/div], **ch3**: rotor speed (sensor) [4 Hz/div], **ch4**: estimated rotor speed (EKF) [4 Hz/div], time scale: 400 ms/div

REFERENCES

[1] T. Orlowska-Kowalska and M. Dybkowski, "Stator-current-based mras estimator for a wide range speed-sensorless induction-motor drive," *Industrial Electronics, IEEE Transactions on*, vol. 57, no. 4, pp. 1296–1308, 2010.

[2] R. Dhaouadi, N. Mohan, and L. Norum, "Design and implementation of an extended Kalman filter for the state estimation of a permanent magnet synchronous motor," *Power Electronics, IEEE Transactions on*, vol. 6, no. 3, pp. 491–497, 1991.

[3] S. Bolognani, R. Oboe, and M. Zigliotto, "Sensorless full-digital PMSM drive with EKF estimation of speed and rotor position.," *IEEE Trans. on Industrial Electronics*, vol. 46, pp. 184 – 191, 1999.

[4] B. Akin, U. Orguner, A. Ersak, and M. Ehsani, "Simple derivative-free nonlinear state observer for sensorless ac drives," *Mechatronics, IEEE/ASME Transactions on*, vol. 11, pp. 634 –643, oct. 2006.

[5] M. Linke, R. Kennel, and J. Holtz, "Sensorless speed and position control of synchronous machines using alternating carrier injection," in *Electric Machines and Drives Conference, 2003. IEMDC'03. IEEE International*, vol. 2, pp. 1211–1217, IEEE, 2003.

[6] J. Holtz and H. Pan, "Acquisition of rotor anisotropy signals in sensorless position control systems," *Industry Applications, IEEE Trans. on*, vol. 40, no. 5, pp. 1379 – 1387, 2004.

[7] R. Leidhold, "Position sensorless control of pm synchronous motors based on zero-sequence carrier injection," *Industrial Electronics, IEEE Transactions on*, vol. 58, pp. 5371 –5379, dec. 2011.

[8] M. Preindl and E. Schaltz, "Sensorless model predictive direct current control using novel second-order pll observer for pmsm drive systems," *Industrial Electronics, IEEE Transactions on*, vol. 58, pp. 4087 –4095, sept. 2011.

[9] D. Vosmik and Z. Peroutka, "Sensorless control of permanent magnet synchronous motor employing extended kalman filter in combination with hf injection method," in *Power Electronics and Applications (EPE 2011), Proceedings of the 2011-14th European Conference on*, pp. 1 –10, 30 2011-sept. 1 2011.

[10] P. F. Driessen, "Dpll bit synchronizer with rapid acquisition using adaptive kalman filtering techniques," *Communications, IEEE Transactions on*, vol. 42, no. 9, pp. 2673–2675, 1994.

[11] A. Patapoutian, "On phase-locked loops and kalman filters," *Communications, IEEE Transactions on*, vol. 47, no. 5, pp. 670–672, 1999.

[12] F. Abry, A. Zgorski, X. Lin-Shi, and J.-M. Retif, "Sensorless position control for spmsm at zero speed and acceleration," in *Power Electronics and Applications (EPE 2011), Proceedings of the 2011-14th European Conference on*, pp. 1 –9, 30 2011-sept. 1 2011.

[13] P. Pillay and R. Krishnan, "Modeling, simulation, and analysis of permanent-magnet motor drives. i. the permanent-magnet synchronous motor drive," *Industry Applications, IEEE Transactions on*, vol. 25, no. 2, pp. 265–273, 1989.

[14] B. Nahid-Mobarakeh, F. Meibody-Tabar, and P. Sargos, "State and disturbance observers in mechanical sensorless control of PMSM," in *Industrial Technology, 2004. IEEE ICIT'04. 2004 IEEE International Conference on*, vol. 1, pp. 181–186, IEEE, 2004.